Kaon decays:

Vision for the future

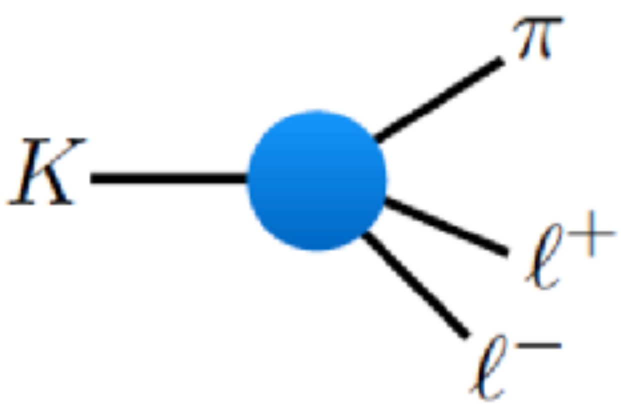

Abhishek U. M. Iyer
Indian Institute of Technology (IIT) Delhi

Rencontres du Vietnam
19 August 2025

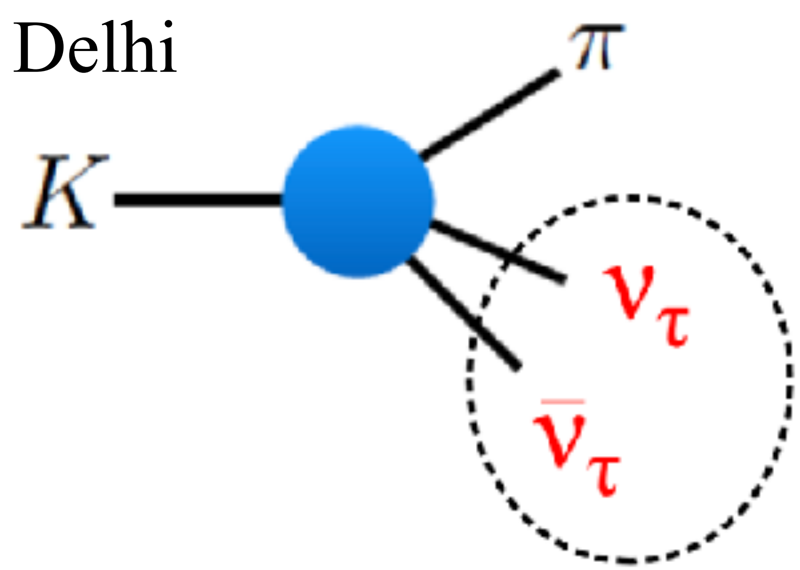

Based on work with G. D'Ambrosio, F. Mahmoudi, S. Neshatpour

Phys.Lett.B 855 (2024) 138824 (2206.14748)
Phys.Rev.D 111 (2025) 1, L011701 (2402.03643)

Bringing Everything together

Most Sensitive to short distance (NP) effects

NA62/KOTO

$K^+ \to \pi^+ \nu\nu$

$K_L \to \pi^0 \nu\nu$

NA62

Scalar operators using $K^+ \to \pi^+ ll$

$K_S \to \mu\mu$ is challenging

New ideas # 2

Kaons

NA62

$K^+ \to \pi^+ ll$

LFUV effects

$$C_9^{sd,\mu} - C_9^{sd,e} = -\frac{a_+^{\mu\mu} - a_+^{ee}}{\sqrt{2} V_{td} V_{ts}^*}$$

KTeV

KOTO2?

$K_L \to \pi^0 ll$

New ideas # 1

Two possible Directions for Future

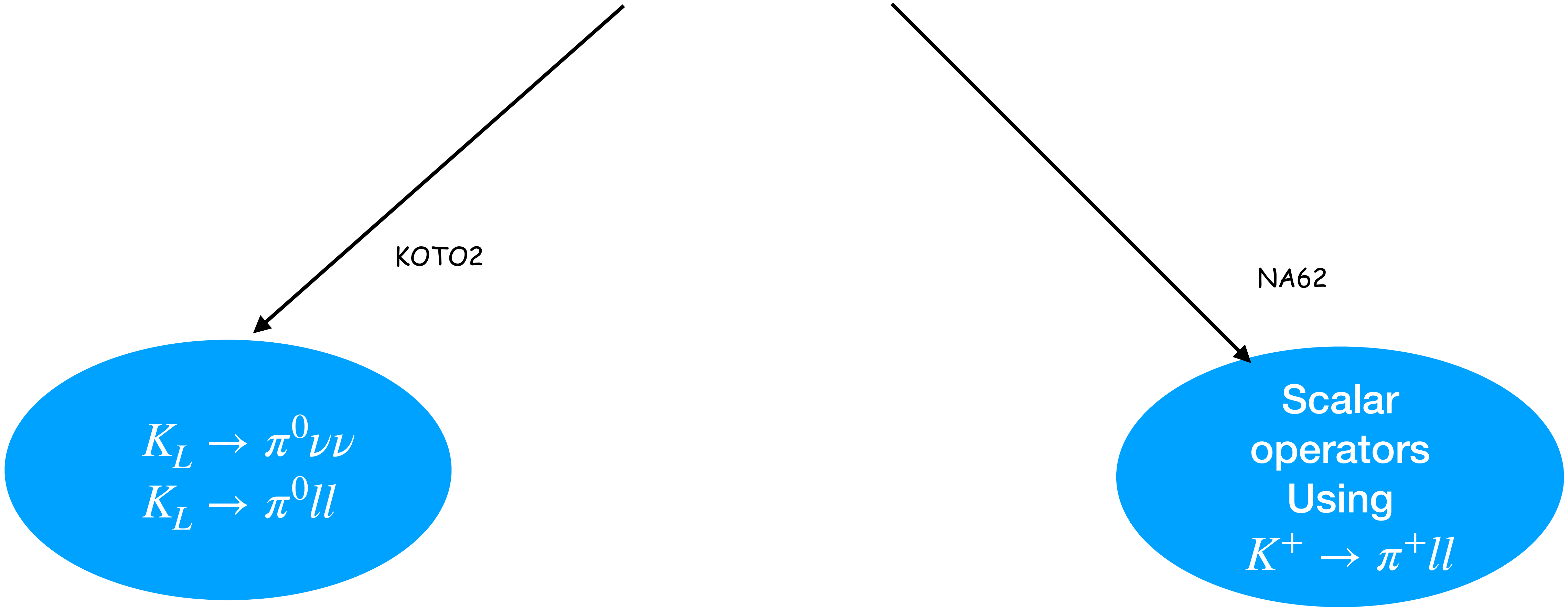

Conventional Beginnings*

The short distance effects (SM +NP) can be parametrised as

Starting Point:

Consider left handed quark currents.

$$\mathcal{H}_{\rm eff} = -\frac{4G_F}{\sqrt{2}}\lambda_t^{sd}\frac{\alpha_e}{4\pi}\sum_k C_k^\ell O_k^\ell \,,$$

$$C_k^\ell = C_{k,\rm SM}^\ell + \delta C_k^\ell$$

$$O_9^\ell = (\bar{s}\gamma_\mu P_L d)\,(\bar{\ell}\gamma^\mu \ell)\,,$$

$$O_{10}^\ell = (\bar{s}\gamma_\mu P_L d)\,(\bar{\ell}\gamma^\mu \gamma_5 \ell)\,,$$

$$O_L^\ell = (\bar{s}\gamma_\mu P_L d)\,(\bar{\nu}_\ell\,\gamma^\mu (1-\gamma_5)\,\nu_\ell)\,,$$

$$\delta C_L^\ell \equiv \delta C_9^\ell = -\delta C_{10}^\ell$$

Charged and neutral leptons are related by $SU(2)_L$ gauge symmetry:
Correlations between different Kaon sectors

*Disclaimer: The terminology "Conventional" is subjective

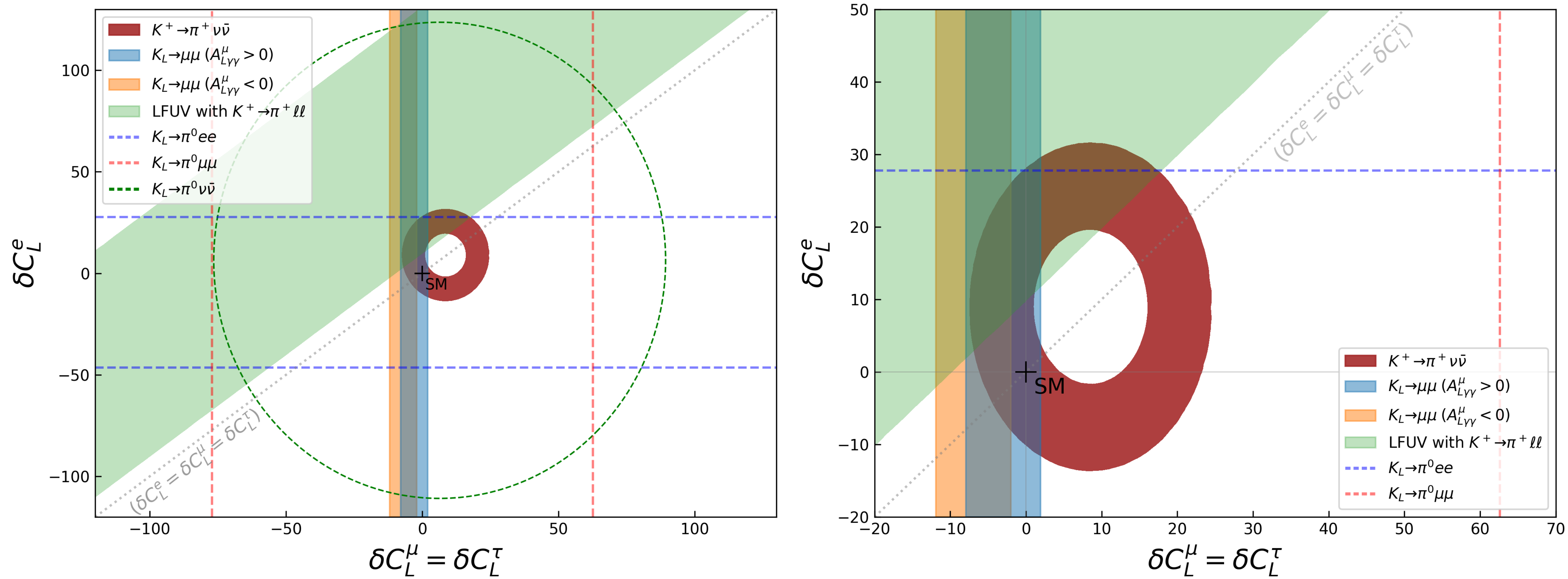

Figure 7. The bounds from individual observables. The right panel is the zoomed version of the left panel. The coloured regions correspond to 68% CL when there is a measurement and the dashed ones to upper limits at 90% CL. $K_L \to \mu\bar{\mu}$ has been shown for both signs of the long-distance contribution. For $K_L \to \pi^0 e\bar{e}$ and $K_L \to \pi^0\mu\bar{\mu}$, constructive interference between direct and indirect CP-violating contributions has been assumed.

D'Ambrosio, A. Iyer, F. Mahmoudi, S. Neshatpour
2206.14748

Kaon Buffet

Observable	SM prediction	Experimental result	Reference	Precision for projections
$\mathrm{BR}(K^+ \to \pi^+ \nu\bar{\nu})$	$(7.86 \pm 0.61) \times 10^{-11}$	$(10.6^{+4.0}_{-3.5} \pm 0.9) \times 10^{-11}$	[1]	15% [23]
$\mathrm{BR}(K_L^0 \to \pi^0 \nu\bar{\nu})$	$(2.68 \pm 0.30) \times 10^{-11}$	$< 1.99 \times 10^{-9}$ @90% CL	[61]	25% [23]
$\mathrm{LFUV}(a_+^{\mu\mu} - a_+^{ee})$	0	-0.014 ± 0.016	[4, 27]	Current
$\mathrm{BR}(K_L \to \mu\bar{\mu})\ (+)$	$(6.82^{+0.77}_{-0.29}) \times 10^{-9}$	$(6.84 \pm 0.11) \times 10^{-9}$	[62]	Current
$\mathrm{BR}(K_L \to \mu\bar{\mu})\ (-)$	$(8.04^{+1.47}_{-0.98}) \times 10^{-9}$			
$\mathrm{BR}(K_S \to \mu\bar{\mu})$	$(5.15 \pm 1.50) \times 10^{-12}$	$< 2.1(2.4) \times 10^{-10}$ @90(95)% CL $\left(0.9^{+0.7}_{-0.6} \times 10^{-10}\right)$	[5]	$< 6.4 \times 10^{-12}$ @95% CL (LHCb@300 fb^{-1} [42, 43])
$\mathrm{BR}(K_L \to \pi^0 e\bar{e})(+)$	$(3.46^{+0.92}_{-0.80}) \times 10^{-11}$	$< 28 \times 10^{-11}$ @90% CL	[17]	25% [23]
$\mathrm{BR}(K_L \to \pi^0 e\bar{e})(-)$	$(1.55^{+0.60}_{-0.48}) \times 10^{-11}$			
$\mathrm{BR}(K_L \to \pi^0 \mu\bar{\mu})(+)$	$(1.38^{+0.27}_{-0.25}) \times 10^{-11}$	$< 38 \times 10^{-11}$ @90% CL	[18]	25% [23]
$\mathrm{BR}(K_L \to \pi^0 \mu\bar{\mu})(-)$	$(0.94^{+0.21}_{-0.20}) \times 10^{-11}$			

Table 1: The SM predictions, current experimental values, and projected precisions. In the last column, "Current" signifies that the measurement precision or the upper bound is maintained at the current experimental level.

Present

$$\chi^2(\delta C_L^\ell) = \sum_{i,j} \left(O_i^{\rm th}(\delta C_L^\ell) - O_i^{\rm exp}\right) C_{i,j}^{-1} \left(O_j^{\rm th}(\delta C_L^\ell) - O_j^{\rm exp}\right)$$

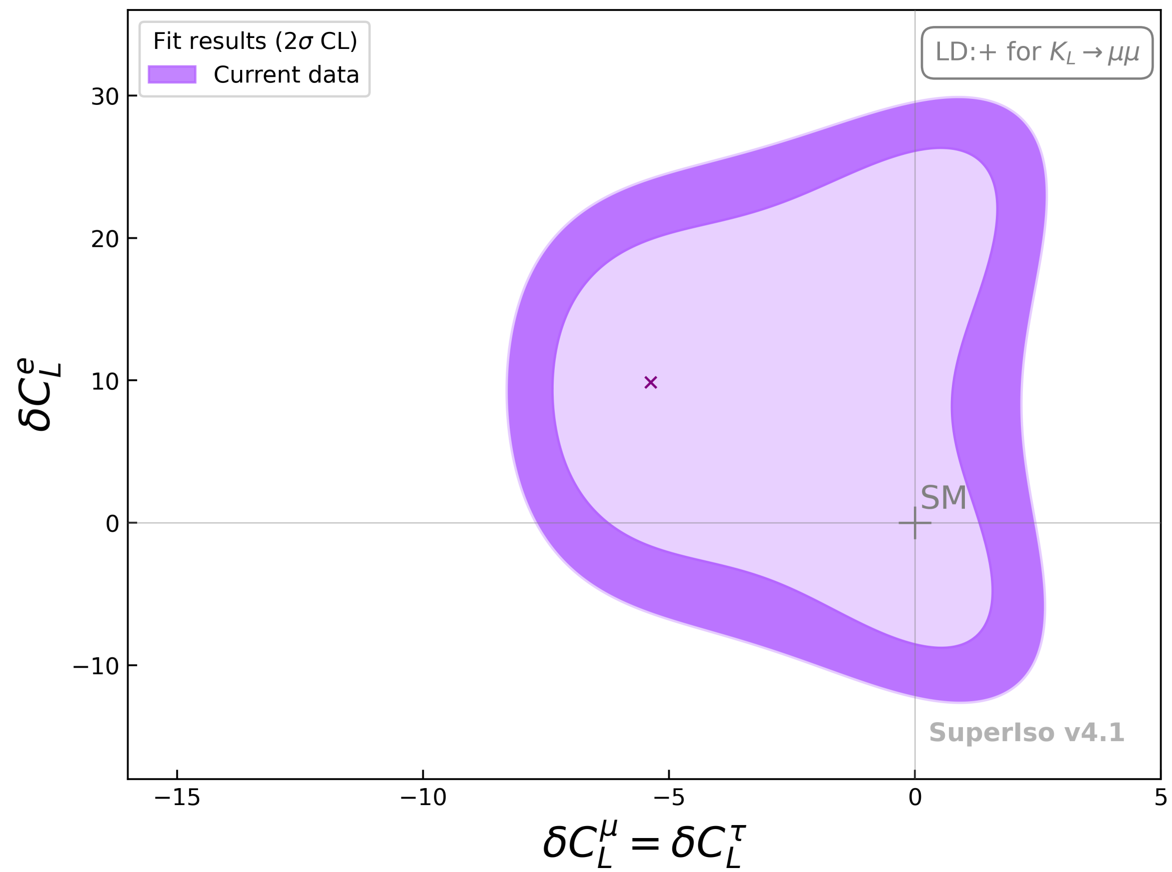

Figure 1: Results of the global fit for the scenario $\delta C_L^\tau = \delta C_L^\mu$ with the best-fit point indicated by the purple cross. The fit is implemented using the existing data with a positive signed long-distance contribution to $K_L \to \mu\bar{\mu}$.

D'Ambrosio, A. Iyer, F. Mahmoudi, S. Neshatpour
2402.03643

Projection!

Two strategies employed

Projection A

For observables with upper bound,
the SM is used as a central values.
For others the same current central value
Is chosen

Projection B

For all observables
best fit values from the existing
global fit is used as central value

The strategy is further simplified by considering three scenarios

Sequential addition of observables, with target precision, to the global analysis

Scenario 1:

$15\,\%$ for $K^+ \to \pi^+\nu\nu$

$25\,\%$ for $K_L \to \pi^0\nu\nu$

↓

Scenario 2:

+ $25\,\%$ for $K_L \to \pi^0 ee$

↓

Scenario 3:

+ $25\,\%$ for $K_L \to \pi^0\mu\mu$

The strategy is further simplified by considering three scenarios

Sequential addition of observables, with target precision, to the global analysis

Scenario 1:

$15\,\%$ for $K^+ \to \pi^+ \nu\nu$

$25\,\%$ for $K_L \to \pi^0 \nu\nu$

↓

Scenario 2:

$+\,25\,\%$ for $K_L \to \pi^0 ee$

↓

Scenario 3:

$+\,25\,\%$ for $K_L \to \pi^0 \mu\mu$

Reminder:

The choice of central values are the two Projections

Scenario 1:

15 % for $K^+ \to \pi^+ \nu\nu$

25 % for $K_L \to \pi^0 \nu\nu$

D'Ambrosio, A. Iyer, F. Mahmoudi, S. Neshatpour
2402.03643

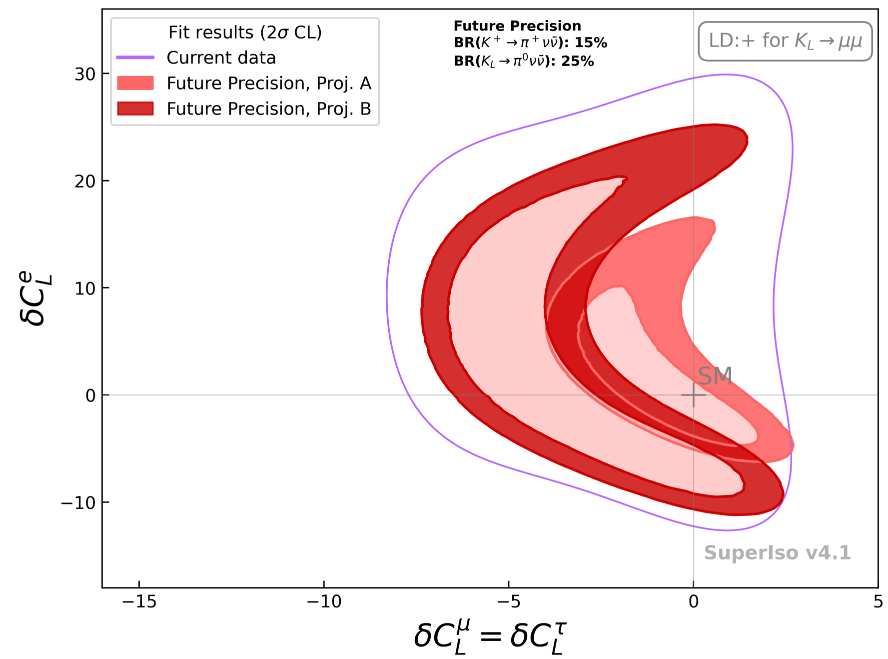

Projection A

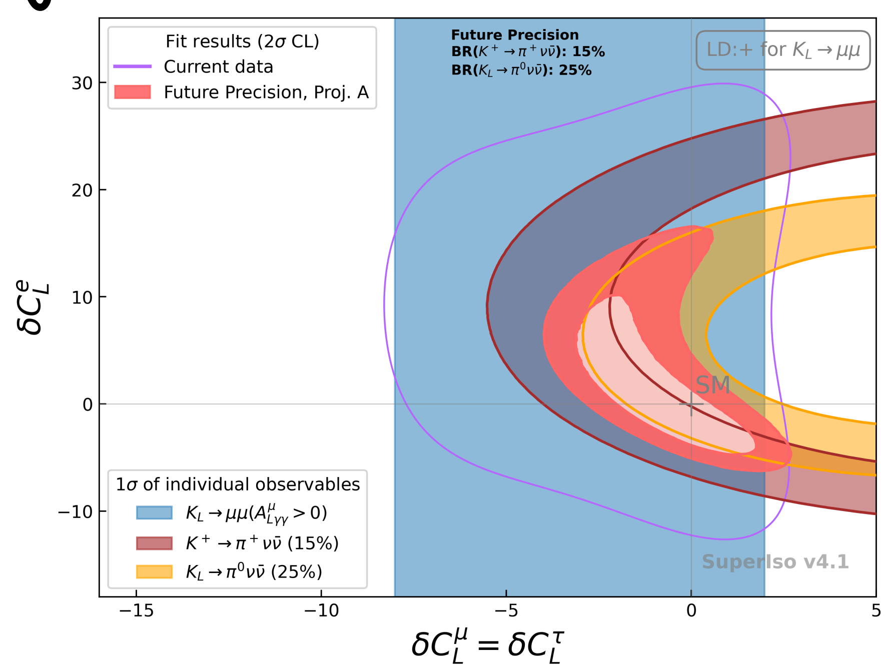

Projection B

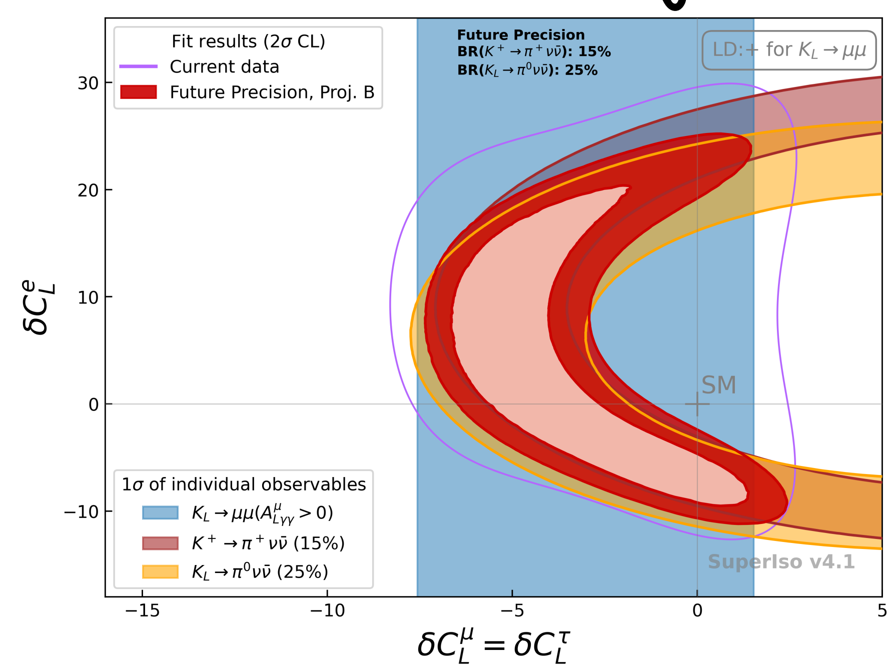

Figure 2: Results corresponding to *Scenario 1*. The top row illustrates the impact on parameter space with the consideration of the golden channels of kaon decays at their projected precisions. The dark (light) red represents 2σ CL regions for Projection A (B). The left (right) plot of the lower row gives the impact of the individual observables on the fit for Projection A (B).

D'Ambrosio, A. Iyer, F. Mahmoudi, S. Neshatpour
2402.03643

Scenario 2:
+ 25 % for $K_L \to \pi^0 ee$

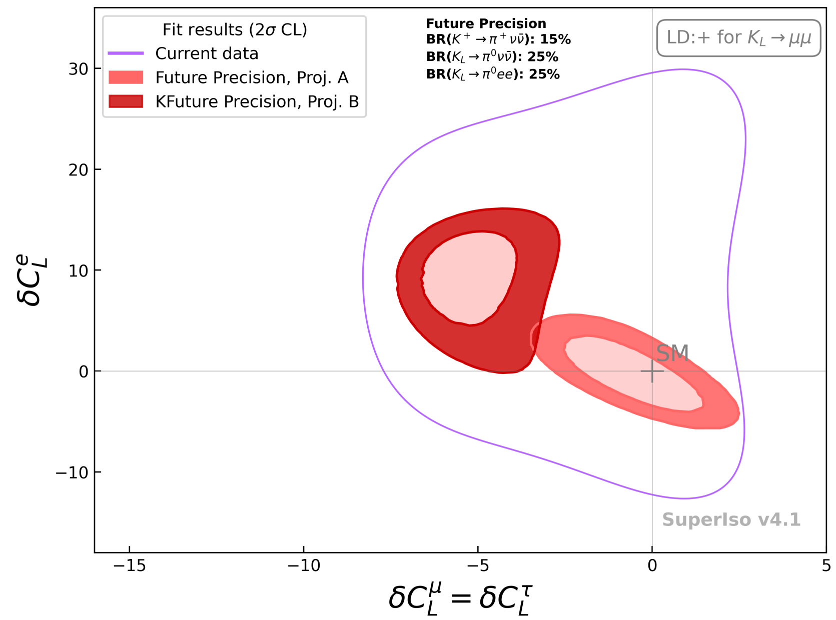

Projection A

Projection B

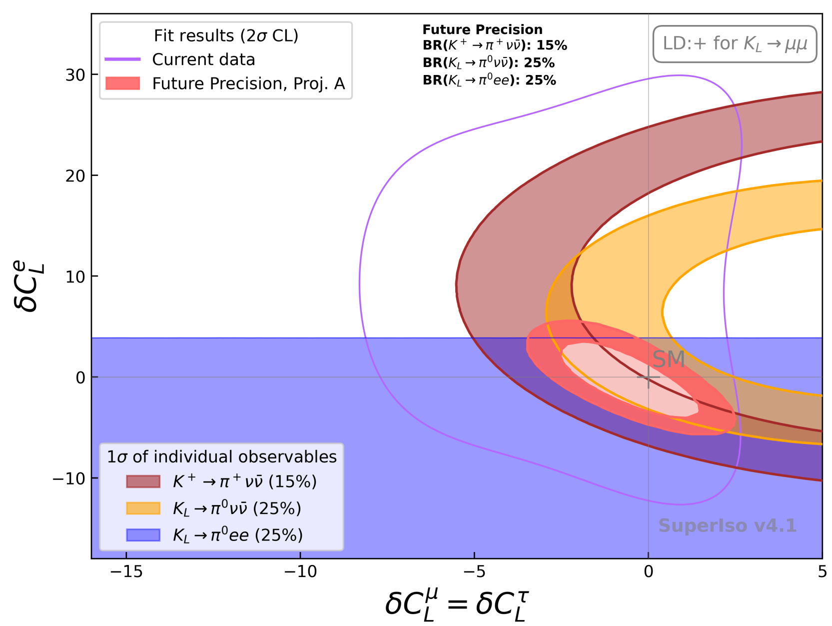

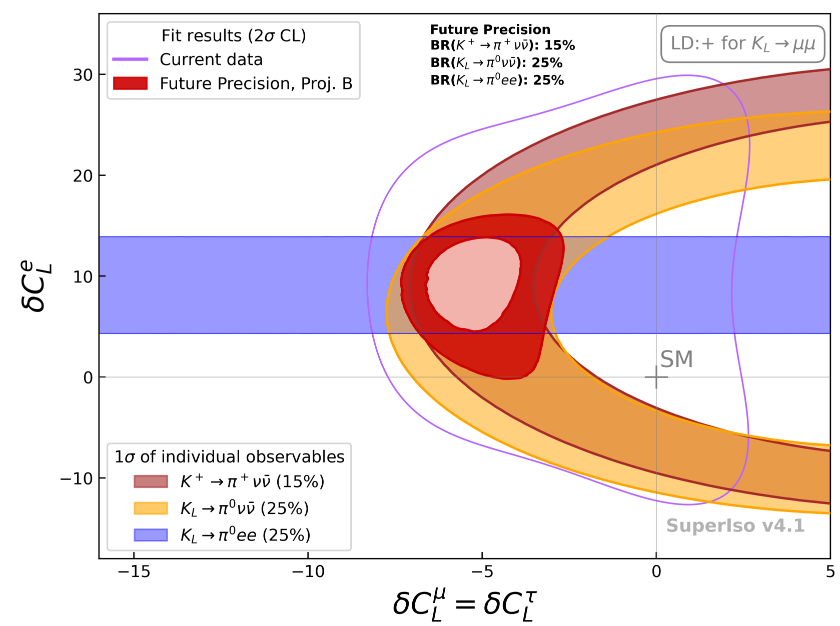

Figure 3: Results corresponding to *Scenario 2*. The top row illustrates the impact on the parameter space with also the inclusion of BR($K_L \to \pi^0 e\bar{e}$) to the fits. The dark (light) red represents 2σ CL regions for Projection A (B). The left (right) plot of the lower row gives the impact of the individual observables on the fit for Projection A (B).

D'Ambrosio, A. Iyer, F. Mahmoudi, S. Neshatpour
2402.03643

Scenario 3:
$+ 25\,\%$ for $K_L \to \pi^0 \mu\mu$

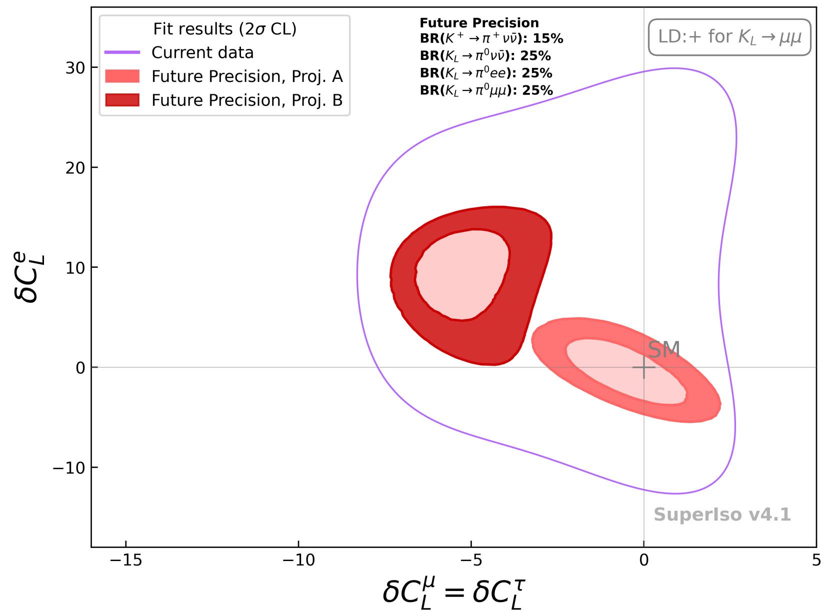

Projection A

Projection B

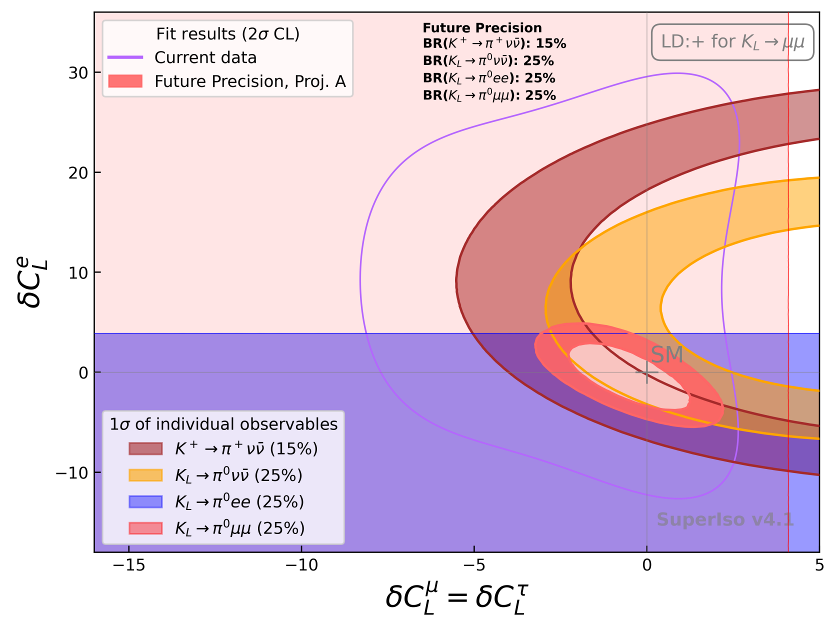

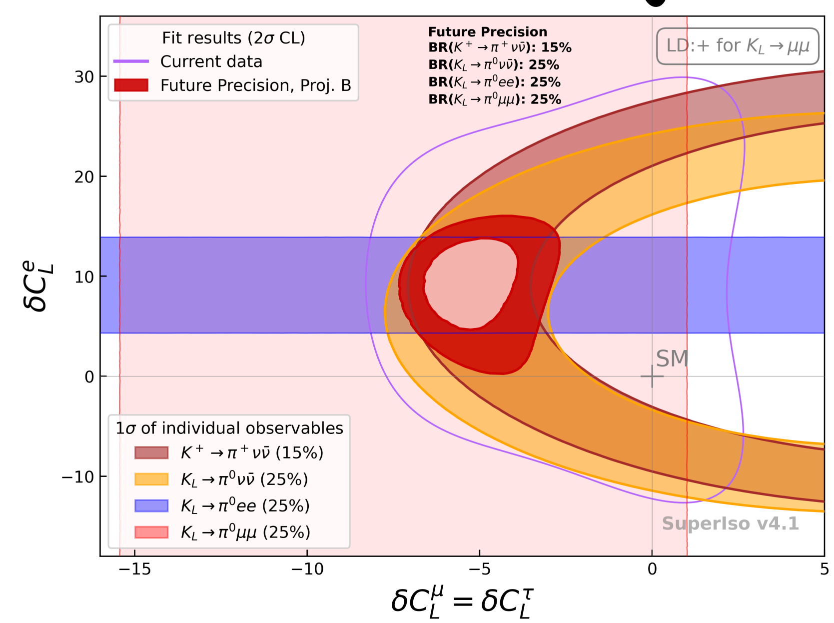

Figure 4: Results corresponding to *Scenario 3*. The top row illustrates the impact on parameters space with also the inclusion of $\mathrm{BR}(K_L \to \pi^0 \mu\bar{\mu})$ to the fits. The dark (light) red represents 2σ CL regions for Projection A (B). The left (right) plot of the lower row gives the impact of the individual observables on the fit for Projection A (B).

Summary 1

Two possible Directions for Future

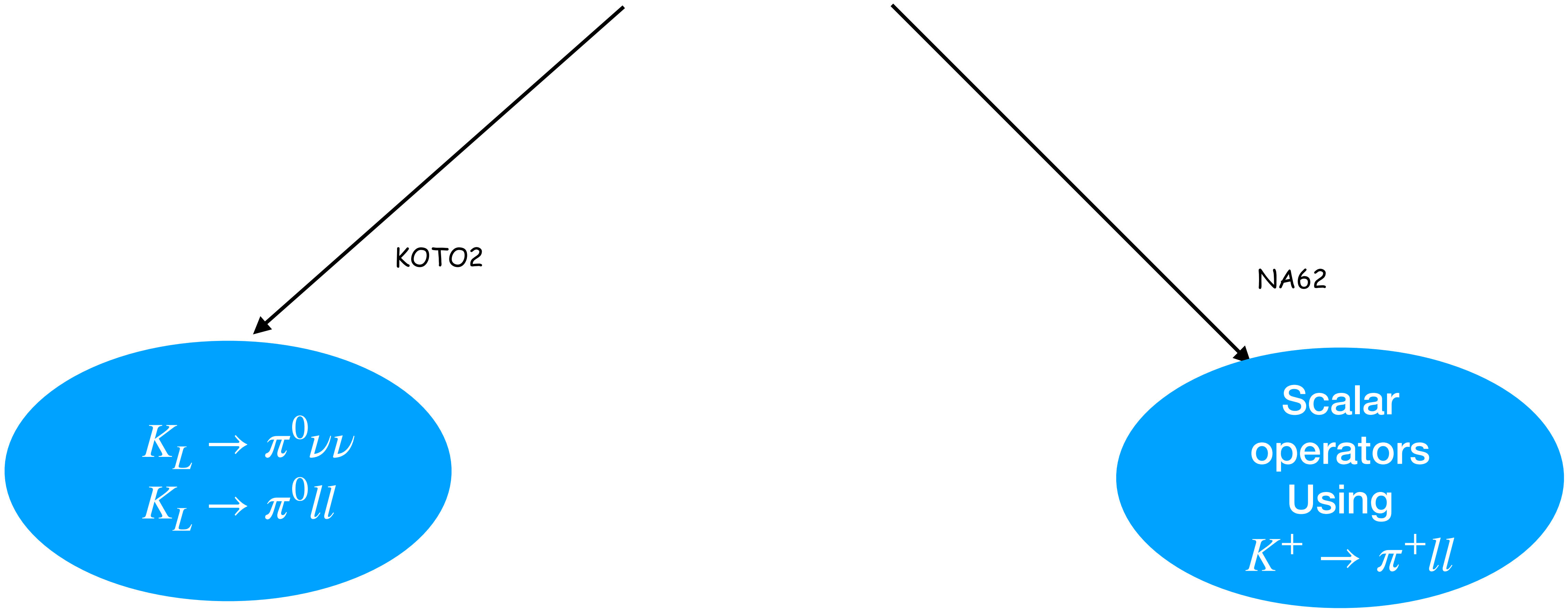

More measurements bring out more features in the parameter space

Disentangling SM and Non-SM like scenarios

For comprehensive fits

D'Ambrosio, A. Iyer, F. Mahmoudi, S. Neshatpour
2206.14748

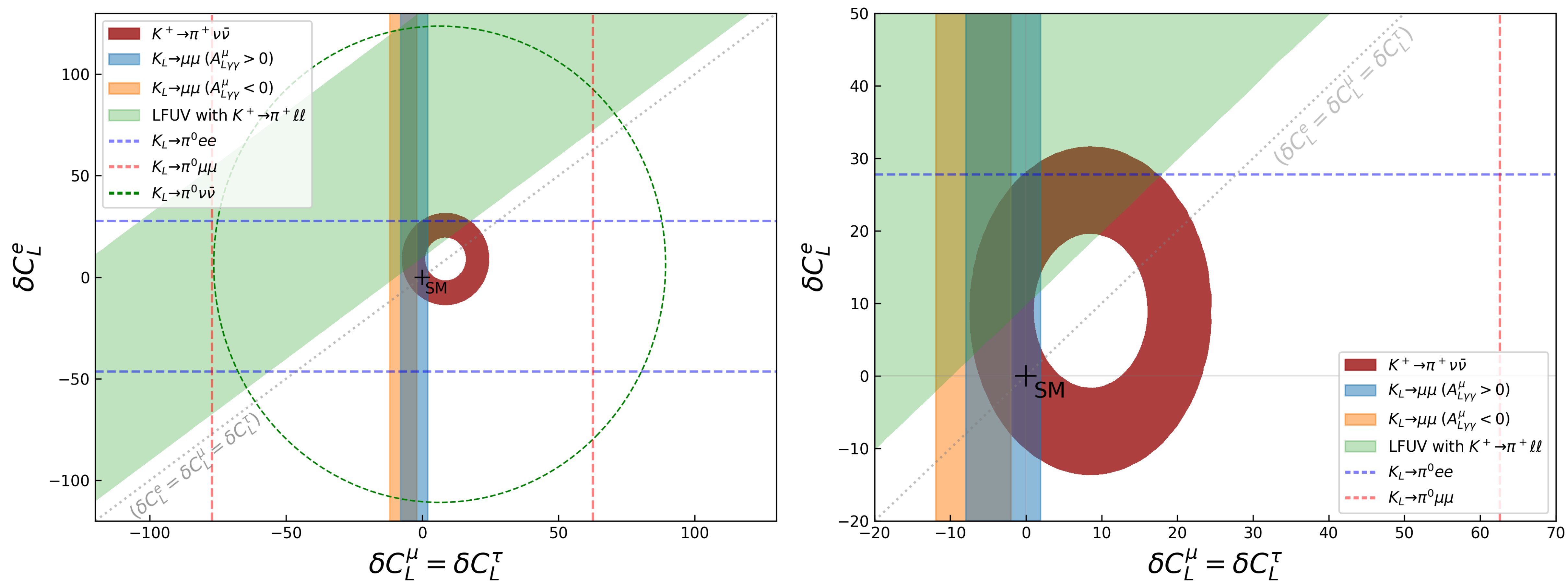

Figure 7. The bounds from individual observables. The right panel is the zoomed version of the left panel. The coloured regions correspond to 68% CL when there is a measurement and the dashed ones to upper limits at 90% CL. $K_L \to \mu\bar{\mu}$ has been shown for both signs of the long-distance contribution. For $K_L \to \pi^0 e\bar{e}$ and $K_L \to \pi^0 \mu\bar{\mu}$, constructive interference between direct and indirect CP-violating contributions has been assumed.

Where is $K_s \to \mu\mu$?

$K_{L,S} \to \mu^+\mu^-$

G. Isidori, Unterdorfer 0311284

$$\mathcal{A}(K^0 \to \ell^+\ell^-) = \bar{u}_\ell(iB + A\gamma_5)v_\ell \ ,$$

$$\mathcal{B}(K^0_{S,L} \to \mu^+\mu^-) = \tau_{S,L}\Gamma(K^0_{S,L} \to \mu^+\mu^-) = \tau_{S,L}\frac{f_K^2 M_K^3 \beta_\mu}{16\pi}\left(|A_{S,L}|^2 + \beta_\mu^2|B_{S,L}|^2\right)$$

Both the `A' and 'B' coefficients receive the SD and LD contributions

The LD for KL is primarily through the A part while KS is through B: CP conserving

SD (CP violating) are necessarily in A for both.

$$\mathrm{BR}(K_S \to \mu\bar{\mu}) = \tau_S \frac{f_K^2 m_K^3 \beta_\mu}{16\pi}\left\{\beta_\mu^2\left|N_S^{\mathrm{LD}}\right|^2 + \left(\frac{2m_\mu}{m_K}\frac{G_F\alpha_e}{\sqrt{2}\pi}\right)^2 \mathrm{Im}^2\left[-\lambda_c\frac{Y_c}{s_W^2} + \lambda_t C_{10}^\ell\right]\right\}, \tag{2.11}$$

LD SD

and for the branching ratio of the $K_L \to \mu\bar{\mu}$ decay we have

$$\mathrm{BR}(K_L \to \mu\bar{\mu}) = \tau_L \frac{f_K^2 m_K^3 \beta_\mu}{16\pi}\left|N_L^{\mathrm{LD}} - \left(\frac{2m_\mu}{m_K}\frac{G_F\alpha_e}{\sqrt{2}\pi}\right)\mathrm{Re}\left[-\lambda_c\frac{Y_c}{s_W^2} + \lambda_t C_{10}^\ell\right]\right|^2, \tag{2.12}$$

(LD+SD)^2

D'Ambrosio, A. Iyer, F. Mahmoudi, S. Neshatpour
2206.14748

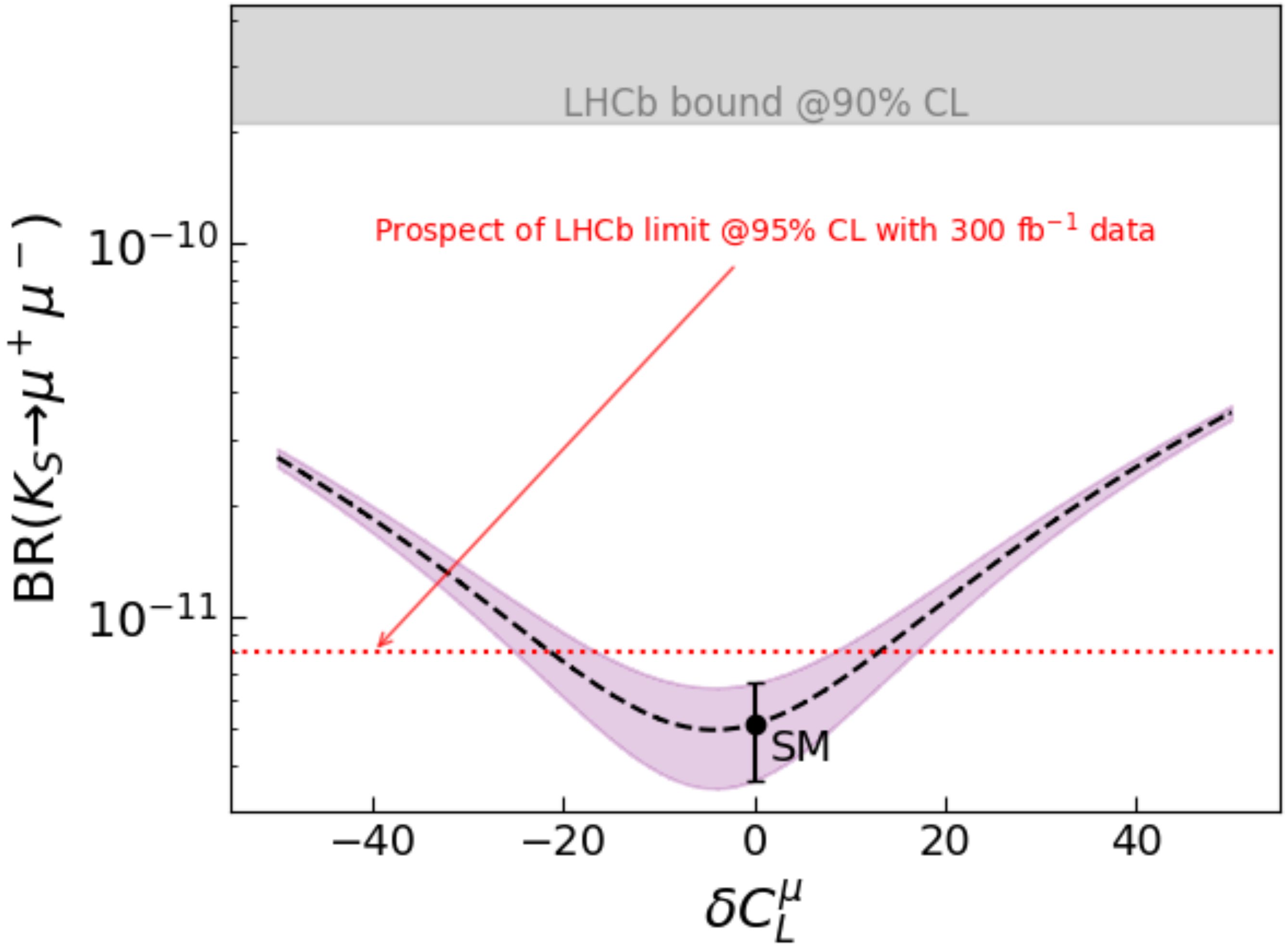

$$\mathrm{BR}(K_S \to \mu\bar{\mu}) = \tau_S \frac{f_K^2 m_K^3 \beta_\mu}{16\pi} \left\{ \beta_\mu^2 \left| N_S^{\mathrm{LD}} \right|^2 + \left(\frac{2m_\mu}{m_K} \frac{G_F \alpha_e}{\sqrt{2}\pi} \right)^2 \mathrm{Im}^2 \left[-\lambda_c \frac{Y_c}{s_W^2} + \lambda_t C_{10}^\ell \right] \right\}, \tag{2.11}$$

Problem: Dominant long distance effects overshadows contributions from C_{10}

One Solution: Add scalar operators → **Not so conventional Beginnings**

One Solution: Add scalar operators → **Not so conventional Beginnings**

$$H_{eff}^{scalar} = C_s \mathcal{O} + \tilde{C}_s \tilde{\mathcal{O}}$$

$$\mathrm{BR}(K_S \to \mu\bar{\mu}) = \tau_S \frac{f_K^2 m_K^3 \beta_\mu}{16\pi} \left\{ \beta_\mu^2 \left| N_S^{\mathrm{LD}} \right|^2 + \left(\frac{2m_\mu}{m_K} \frac{G_F \alpha_e}{\sqrt{2}\pi} \right)^2 \mathrm{Im}^2 \left[-\lambda_c \frac{Y_c}{s_W^2} + \lambda_t C_{10}^{\ell} \right] \right\}, \quad (2.11)$$

$$B_S = N_S^{\mathrm{LD}} - \frac{m_s M_K}{m_s + m_d} \mathrm{Re}(C_S - \tilde{C}_S)$$

Question: What are ways to get a handle on the scalar contributions?

One Solution: Lets go back to $K^+ \to \pi^+ ll$

$$\frac{d\Gamma}{dz} = \frac{2}{3}\frac{G_F^2 M_K^5}{2^8\pi^3}\beta_\ell \lambda^{1/2}(z)$$

$f_V \propto a + bz + V^{\pi\pi}$

SM

$$\times \left\{ |f_V|^2 \, 2\frac{\alpha^2}{16\pi^2}\lambda(z)\left(1+2\frac{r_\ell^2}{z}\right)\right.$$

NOT SM

$$\left. + |f_S|^2 \, 3\, z\beta_\ell^2 \right\} .$$

$$H_{eff}^{scalar} = C_s \mathcal{O} + \tilde{C}_s \tilde{\mathcal{O}}$$

Chen et al 0302207

Gao 0311253

Chen et al 0302207
Gao 0311253

$$\frac{d^2\Gamma}{dz\, d\cos\theta} = \frac{G_F^2 M_K^5}{2^8\pi^3}\beta_\ell\, \lambda^{1/2}(z) \times \left\{ |f_V|^2 \frac{\alpha^2}{16\pi^2}\lambda(z)(1-\beta_\ell^2\cos^2\theta) + |f_S|^2 z\beta_\ell^2 + \mathrm{Re}(f_V^* f_S)\frac{\alpha\, r_\ell}{\pi}\beta_\ell\lambda^{1/2}(z)\cos\theta \right\},$$

There is more

$$A_{\rm FB}(z) = \frac{\alpha G_F^2 M_K^5}{2^8\pi^4} r_\ell\, \beta_\ell^2(z)\lambda(z)\mathrm{Re}\left(f_V^* f_S\right) \Big/ \left(\frac{d\Gamma(z)}{dz}\right),$$

$\propto m_l$

Difficult to do this for the electron mode.

A_{FB}

$$A_{FB}(z) = \frac{\frac{\alpha G_F^2 M_K^5}{2^8\pi^4} r_\ell \, \beta_\ell^2(z)\lambda(z)\mathrm{Re}\left(f_V^* f_S\right)}{\left(\frac{d\Gamma(z)}{dz}\right)}$$

BR

$$\frac{d\Gamma}{dz} = \frac{2}{3}\frac{G_F^2 M_K^5}{2^8\pi^3}\beta_\ell \lambda^{1/2}(z) \times \left\{ |f_V|^2 \, 2\frac{\alpha^2}{16\pi^2}\lambda(z)\left(1+2\frac{r_\ell^2}{z}\right) + |f_S|^2 \, 3\, z\beta_\ell^2 \right\}.$$

Central value

Error Piece

$(K^+ \to \pi^+\mu^+\mu^-)$		
NA48	exp	$\lvert f_S\rvert <$
$A_{\rm FB}$	$(-2.4 \pm 1.8) \times 10^{-2}$	4.2×10^{-5}
BR	$(9.62 \pm 0.21) \times 10^{-8}$	1.0×10^{-4}
NA62	exp	$\lvert f_S\rvert <$
$A_{\rm FB}$	$(0.0 \pm 0.7) \times 10^{-2}$	7.7×10^{-6}
BR	$(9.16 \pm 0.06) \times 10^{-8}$	5.6×10^{-5}

$(K^+ \to \pi^+e^+e^-)$		
E865	exp	$\lvert f_S\rvert <$
$A_{\rm FB}$	–	–
BR	$(2.988 \pm 0.040) \times 10^{-7}$	6.8×10^{-5}
NA48	exp	$\lvert f_S\rvert <$
$A_{\rm FB}$	–	–
BR	$(3.14 \pm 0.04) \times 10^{-7}$	6.8×10^{-5}

TABLE I. Bound on f_S at 90% CL, from $A_{\rm FB}$ and the uncertainty of the branching ratio. In each panel, the last column corresponds to the upper bound obtained from the experimental measurement of the column to its left. For the electron channel, there are no measurements for the forward-backward asymmetry.

D'Ambrosio, A. Iyer, F. Mahmoudi, S. Neshatpour
2404.03643

D'Ambrosio, A. Iyer, F. Mahmoudi, S. Neshatpour
2404.03643

A three parameter fit

	$d\Gamma/dz$	$A_{\rm FB} + d\Gamma/dz$
$K \to \pi ee$	$\lvert f_S\rvert <$	$\lvert f_S\rvert <$
E865	8.0×10^{-5}	–
NA48/2	4.0×10^{-5}	–
$K \to \pi\mu\mu$	$\lvert f_S\rvert <$	$\lvert f_S\rvert <$
NA48/2	10.0×10^{-5}	4.1×10^{-5}
NA62	9.0×10^{-5}	7.9×10^{-6}

Similar to A_{FB} only bound
$f_s < 7.7 \times 10^{-6}$

TABLE II. Upper bound for f_S at 90% CL, from the three parameter fit to a, b and f_S using various datasets. For the relevant inputs regarding the theoretical calculations we have considered PDG 2022 [15], and the external parameters α_+, β_+ are taken from [16], in agreement with NA62 [14].

D'Ambrosio, A. Iyer, F. Mahmoudi, S. Neshatpour
2404.03643

Bound from the fit

$$f_s < 7.9 \times 10^{-6}$$

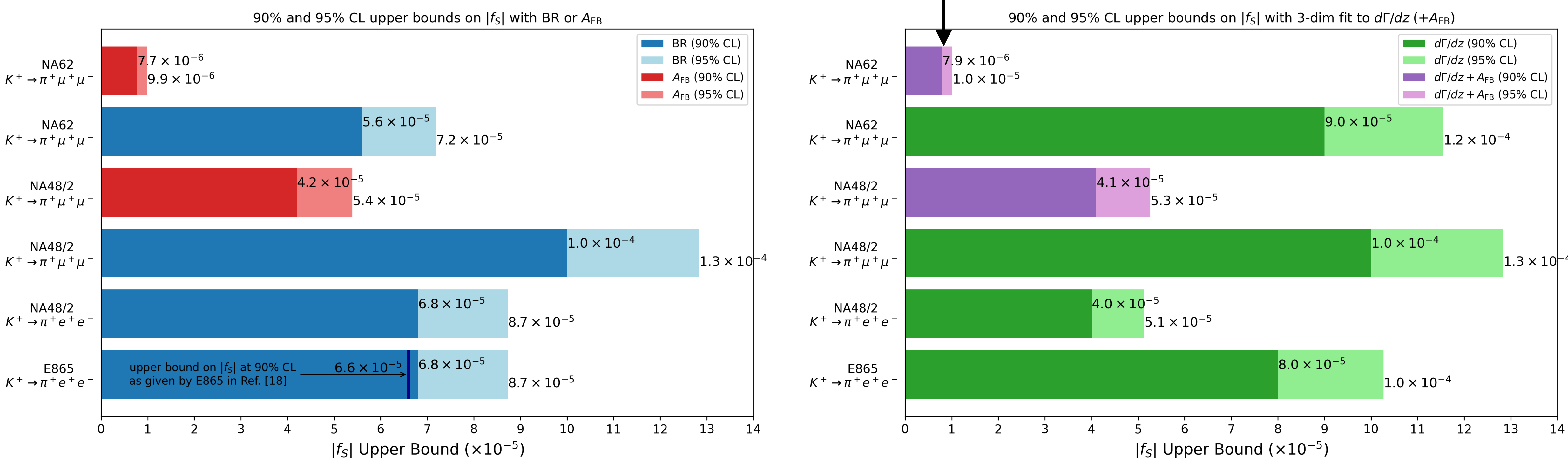

Figure 1: The 90% and 95% CL upper bound on $|f_S|$ obtained by our analysis of different experimental datasets. Left: bound from BR or $A_{\rm FB}$ as given in Table 1. Right: bound from 3-dim. fit to f_V and f_S as given in Table 2. The vertical black line in the left plot corresponds to the only existing experimental upper bound from E865 [18].

Overall Summary

Two possible Directions for Future

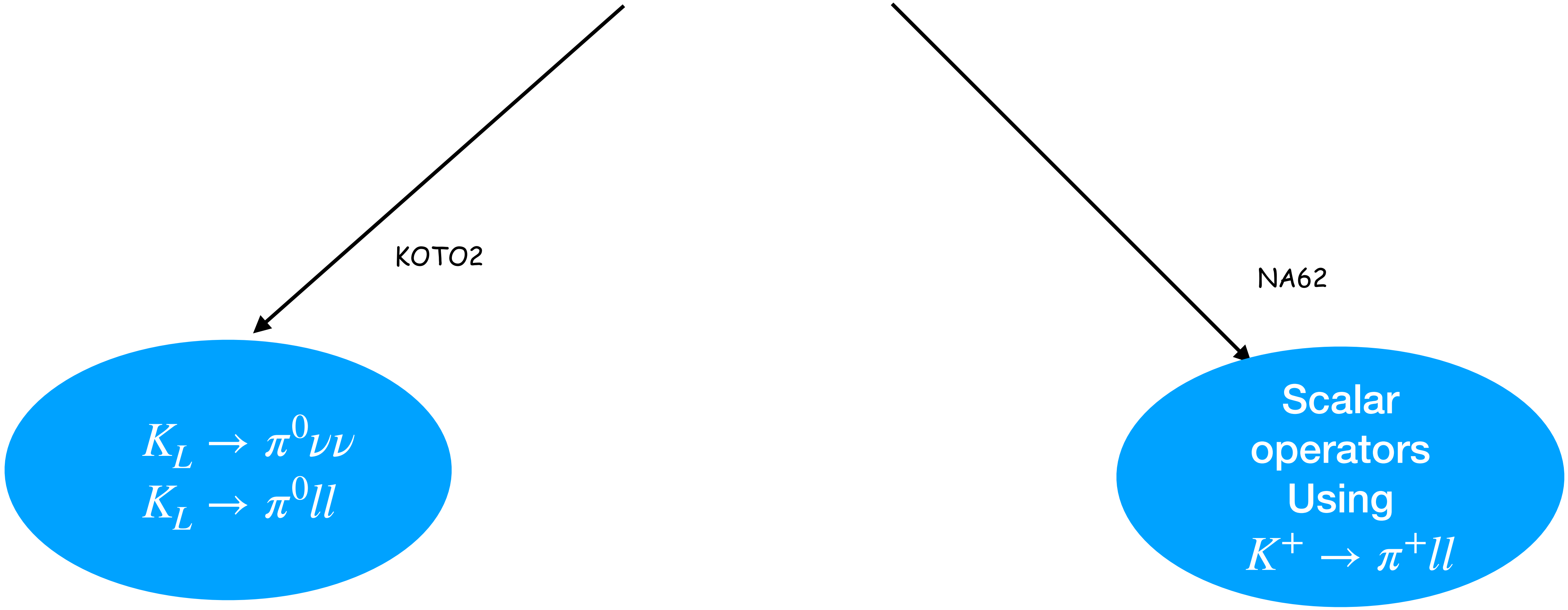

More measurements bring out more features in the parameter space

Disentangling SM and Non-SM like scenarios

$K_S \to \mu\mu$ naturally motivates the consideration of scalar operators

Bound from the fit

$$f_s < 7.9 \times 10^{-6}$$

Looking forward…

Wishlist: More Experimental inputs from $K^+ \to \pi^+ \mu\mu$ and $K^+ \to \pi^+ ee$

To do:

Follow `unconventional' routes for Kaon physics

Humanyun's Tomb
New Delhi

iyerabhishek@physics.iitd.ac.in

Thank you!